Phase separation of hydrogen atoms adsorbed on graphene and the smoothness of the graphene-graphane interface

A. L. Rakhmanov, A. V. Rozhkov, A. O. Sboychakov, and Franco Nori

Phase separation of hydrogen atoms adsorbed on graphene and the smoothness of the graphene-graphane interface

A.L. Rakhmanov,[1,2] A.V. Rozhkov,[1,2] A.O. Sboychakov,[1,2] and Franco Nori[1,3]

[1]*Advanced Science Institute, RIKEN, Wako-shi, Saitama, 351-0198, Japan*
[2]*Institute for Theoretical and Applied Electrodynamics,*
Russian Academy of Sciences, 125412 Moscow, Russia
[3]*Department of Physics, University of Michigan, Ann Arbor, MI 48109-1040, USA*

The electronic properties of a graphene sheet with attached hydrogen atoms is studied using a modified Falicov-Kimball model on the honeycomb lattice. It is shown that in the ground state this system separates into two phases: fully hydrogenated graphene (graphane) and hydrogen-free graphene. The graphene-graphane boundary acquires a positive interface tension. Therefore, the graphene-graphane interface becomes a straight line, slightly rippled by thermal fluctuations. A smooth interface may be useful for the fabrication of mesoscopic graphene-based devices.

I. INTRODUCTION

Creating a sample with flat edges is a significant challenge for producing graphene mesoscopic devices[1–3]. One possibility is to break a graphene sheet into fragments with sharp edges.[4] Another alternative involves the use of graphane. Graphane[5] is fully hydrogenated graphene; it is an insulator with a gap of several eV. With graphane, instead of physically cutting graphene, one can create graphene patches of required shapes inside a sheet of graphane by local de-hydrogenation. In such systems, low-energy electrons from graphene cannot penetrate the insulating graphane host. Therefore, the graphene-graphane interface serves as the effective edge of the graphene structure. Different arrangements of this type have been discussed.[6,7] Thus, the issue of the graphene-graphane interface stability is important both for fundamental and applied research. There are indications from numerical studies that such interface is stable[8,9], and that the adsorbed hydrogens tend to cluster together.[10] This tendency may be explained in terms of phase separation into hydrogen-rich and hydrogen-free regions. This separation was established on the basis of a semi-phenomenological analysis of electron-mediated interactions between hydrogen adatoms in graphene.[11]

The purpose of the present paper is twofold. First, we put forward a microscopic approach to the problem of phase separation in graphene-graphane systems. To demonstrate the phase separation, Ref. 11 assumed a specific type of interaction between the graphene electrons and the adatoms. For the hydrogen adatoms this assumption is supported experimentally and numerically. However, it remains unclear if the phase separation is a unique feature of the hydrogen on graphene, or other adsorbents would show the same feature. Avoiding phenomenological arguments, we discuss the phase separation within the framework of a modified Falicov-Kimball model, with an infinite interaction constant between 'a hydrogen hole' and an s-electron on the hydrogen atom. The advantage of such an approach is its generality: the

phase separation is a known property of a ground state of Falicov-Kimball-like models[12–16] robust against variation of microscopic details. To estimate the characteristic energies of the phase-separated state, we apply the Hubbard-I approximation.[17] To check the validity of this approximation, we also perform exact diagonalizations of the model Hamiltonian in a finite cluster.

The phase separation implies that the homogeneous state is either unstable or metastable. However, it is possible to imagine that, under suitable conditions, such phase may be stabilized for a long period of time. If the stabilization is indeed possible, the properties of the homogeneous phase can be investigated. Our calculations show that the homogeneous phase has finite density of states at the Fermi energy, in agreement with the numerical results of Ref. 10.

Our second goal is to explore the connection between phase separation and the stability of the graphene-graphane interface. We show that the graphene-graphane interface has a positive boundary tension. To stretch the interface with a positive interface tension by a unit length requires a finite amount of work. This amount is high for the system considered. Thus, the interface remains flat over substantial distances, which is a highly desired property, necessary for the creation of ballistic mesoscopic systems. In other words, the interface is stable not only with respect to vacancy defects in small samples, as found in Refs. 8 and 9, but also with respect to any conceivable defect. Our approach allows to obtain a qualitative estimate of the interface tension and to assess the flatness of the interface at a given temperature. We estimate that at room temperature the graphene-graphane interface remains atomically smooth over distances of about 10^2 lattice constants.

The paper is organized as follows. In Sec. II we formulate the model of the adatoms adsorbed on a graphene sample. This model is solved in Sec. III within the Hubbard-I approximation. To check the accuracy of the Hubbard-I approximation a finite-cluster numerical study is presented in Sec. IV. In Sec. V we investigate

the stability of the graphene-graphane interface, evaluate the interface tension, and investigate its smoothness. The conclusions are given in Sec. VI.

II. MODEL

We use the model Hamiltonian for graphane:

$$H_{\rm A} = H_{\rm E} - \sum_{i\sigma} \left[t_0 \left(P_{i\sigma}^\dagger S_{i\sigma} + {\rm h.c.} \right) + \varepsilon_{\rm H} S_{i\sigma}^\dagger S_{i\sigma} \right], \quad (1)$$

$$H_{\rm E} = - \sum_{ij\sigma} \left(P_{i\sigma}^\dagger \hat{T}_{ij} P_{j\sigma} + {\rm h.c.} \right), \quad (2)$$

where $P_{i\sigma}^\dagger = \left(p_{i\sigma}^{\mathcal{A}\dagger}, p_{i\sigma}^{\mathcal{B}\dagger} \right)$, $S_{i\sigma}^\dagger = \left(s_{i\sigma}^{\mathcal{A}\dagger}, s_{i\sigma}^{\mathcal{B}\dagger} \right)$, σ is the spin projection. The Hamiltonian $H_{\rm E}$ ($H_{\rm A}$) corresponds to graphene (graphane). Below, label 'E' ('A') is used to denote quantities associated with graphEne (graphAne). The Hamiltonian $H_{\rm E}$ is the usual graphene Hamiltonian corresponding to p_z-electrons of carbon hopping between nearest carbon atoms arranged into the honeycomb lattice. For such lattice, the electron creation operators are arranged into a spinor $P_{i\sigma}^\dagger$, where i denotes the biatomic unit cell of the lattice. The spinor component labeled '$\mathcal{A}$' ('$\mathcal{B}$') corresponds to a site on the $\mathcal{A}$ sublattice ($\mathcal{B}$ sublattice). The hopping matrix $\hat{T}_{ij}$ in the spinor representation in momentum space is

$$\hat{T}_{\bf k} = \begin{pmatrix} 0 & t_{\bf k} \\ t_{\bf k}^* & 0 \end{pmatrix},$$

$$t_{\bf k} = t_p \left[1 + 2 \exp\left(\frac{3ik_x a_0}{2} \right) \cos\left(\frac{\sqrt{3}k_y a_0}{2} \right) \right]. \quad (3)$$

The Hamiltonian $H_{\rm A}$ is a simplified model of graphane. It describes the p_z-electrons of graphene hybridized with the s-electrons of hydrogen, attached to each carbon atom. Other bands are disregarded. The carbon-hydrogen hybridization constant $t_0 = 5.8\,{\rm eV}$ exceeds the carbon-carbon hopping amplitude $t_p = 2.8\,{\rm eV}$ and the relative energy of the hydrogen s-orbital $\varepsilon_{\rm H} = 0.4\,{\rm eV}$.[7]

In **k**-space the Hamiltonian $H_{\rm A}$ can be expressed as

$$H_{\rm A} = \begin{pmatrix} \hat{T}_{\bf k} & t_0 \sigma_0 \\ t_0 \sigma_0 & \varepsilon_{\rm H} \sigma_0 \end{pmatrix}, \quad (4)$$

where σ_0 is the 2x2 unity matrix. Here the upper left 2x2 corner corresponds to the carbons atoms, lower right 2x2 block corresponds to the hydrogens, the remaining blocks describe the C-H hopping.

The matrix for $H_{\rm A}$ is easy to diagonalize. As a result we obtain four graphane bands:

$$\varepsilon_m^{\rm A} = \frac{1}{2} \left(\pm |t_{\bf k}| \pm \sqrt{4t_0^2 + |t_{\bf k}|^2} \right), \quad m = 1, 2, 3, 4. \quad (5)$$

In this formula $\varepsilon_{\rm H}$ is neglected for it is small.

Although only four bands in graphane are considered in our model Hamiltonian, Eq. (1), it captures the main features of graphane: at half filling, Eq. (1) describes an insulator with a gap located at the Γ point. The value of the gap E_g (for the parameters written above $E_g = 6.0\,{\rm eV}$) is found to be consistent with Ref. 18,19. Note, however, that there is no consensus about the exact values of the graphane model parameters. But high precision is not important for the qualitative results obtained below.

The Hamiltonian $H_{\rm A}$ is valid when the numbers of hydrogen and carbon atoms are equal. If at some site hydrogen is absent, then the hydrogen s-orbital is not available for the electrons. This constraint may be enforced by introducing an infinitely-strong repulsion between the "hydrogen hole" and the electron on the s-orbital:

$$H_{\rm EA} = H_{\rm A} + U \sum_{i\sigma} S_{i\sigma}^\dagger \widehat{N}_i^{\rm hh} S_{i\sigma}, \quad (6)$$

$$\widehat{N}_i^{\rm hh} = {\rm diag}(n_{\mathcal{A}i}^{\rm hh}, n_{\mathcal{B}i}^{\rm hh}), \quad (7)$$

where $U \to +\infty$, and $n_{\mathcal{A},\mathcal{B}i}^{\rm hh}$ are the numbers of hydrogen holes at site i. These numbers can randomly take the values 0 or 1 with mean value $\langle n_{\mathcal{A},\mathcal{B}i}^{\rm hh} \rangle = n^{\rm hh}$, where $n^{\rm hh}$ is the concentration of hydrogen holes per carbon atom. The Hamiltonian $H_{\rm EA}$ is a version of the Falicov-Kimball model in which mobile p- and s-electrons interact with immobile "holes" whose concentration $n^{\rm hh}$ is fixed externally. Thus, $n^{\rm hh} = 1$ refers to graphene, $n^{\rm hh} = 0$ refers to graphane. Below, we will study partial hydrogenation: $0 < n^{\rm hh} < 1$.

III. CALCULATIONS

An analogy between $H_{\rm EA}$, Eq. (6), and the Falicov-Kimball model is very useful for our purposes since the latter model experiences phase separation in a broad range of parameters.[12–16] The reasons for the existence of phase separation here can be understood with the help of simple arguments. Since t_0 exceeds t_p, let us study the limit

$$t_0 \gg t_p. \quad (8)$$

We now introduce the electron operators a, b diagonalizing those terms of $H_{\rm EA}$ which do not involve the carbon-carbon hopping:

$$H_{\rm EA} - H_{\rm E} = \sum_\alpha a_\alpha^\dagger a_\alpha \left[t_0(1 - n_\alpha^{\rm hh}) + U n_\alpha^{\rm hh} \right]$$
$$- t_0 \sum_\alpha b_\alpha^\dagger b_\alpha (1 - n_\alpha^{\rm hh}), \quad (9)$$

where

$$p_\alpha = \frac{b_\alpha - a_\alpha}{\sqrt{2}} (1 - n_\alpha^{\rm hh}) + n_\alpha^{\rm hh} b_\alpha,$$

$$s_\alpha = \frac{b_\alpha + a_\alpha}{\sqrt{2}} (1 - n_\alpha^{\rm hh}) + n_\alpha^{\rm hh} a_\alpha. \quad (10)$$

We omit the sublattice and spin labels since the expressions are the same for any $\mathcal{A}, \mathcal{B}$, and σ. The index α labels individual carbon atoms (i, j label unit cells). In Eq. (9) we neglect the term proportional to ε_H since $\varepsilon_\mathrm{H} \ll t_p$ ($\ll t_0$). It follows from Eq. (9) that the on-site energy of the fermions a is much higher than the on-site energy of b for any n_α^hh, since $t_0, U \gg t_p$. Thus, to lowest order in t_p/t_0, these states are empty, and can be neglected. In this approximation

$$H_\mathrm{EA} \approx -t_0 \sum_\alpha b_\alpha^\dagger b_\alpha (1 - n_\alpha^\mathrm{hh})$$

$$-\frac{t_p}{2} \sum_{\langle \alpha\beta \rangle} b_\alpha^\dagger b_\beta [1 + \gamma(n_\alpha^\mathrm{hh} + n_\beta^\mathrm{hh}) + \gamma^2 n_\alpha^\mathrm{hh} n_\beta^\mathrm{hh}], \quad (11)$$

$$\gamma = \sqrt{2} - 1 \approx 0.41, \quad (12)$$

where $\langle \ldots \rangle$ denotes summation over the nearest neighbors. From this equation we see that to separate two hydrogen holes sitting on neighboring sites one must spend an energy of the order of $t_p \gamma^2 \langle b_\alpha^\dagger b_\beta \rangle$. This corresponds to the *attraction* between the hydrogen holes (and between the hydrogen atoms) as in the model used in Ref. 11. This attraction induces the phase separation. The additional correlations between the adsorbed adatoms (e.g., due to bond reorganization in graphane), which our model neglects, may be incorporated as an effective short-range attraction between the hydrogens. The effect of this attraction is obvious: it favors phase separation.

Using H_EA, Eq. (6), we can derive the equation of motion for the single-electron Green's function in the $(\omega, \mathbf{k})$ representation:

$$(\omega + \mu)\hat{G}_{pp} + \hat{T}_\mathbf{k}\hat{G}_{pp} + t_0\hat{G}_{sp} = 1,$$
$$(\omega + \mu + \varepsilon_\mathrm{H})\hat{G}_{sp} + t_0\hat{G}_{pp} - U\hat{F}_{sp} = 0. \quad (13)$$

Here μ is the chemical potential, $\hat{G}_{pp,sp}$ and $\hat{F}_{sp}$ are the Fourier transforms of the time-ordered propagators

$$\hat{G}_{pp}(i-j,t) = -i\left\langle T\, P_{i\sigma}(t)P_{j\sigma}^\dagger(0) \right\rangle,$$
$$\hat{G}_{sp}(i-j,t) = -i\left\langle T\, S_{i\sigma}(t)P_{j\sigma}^\dagger(0) \right\rangle, \quad (14)$$
$$\hat{F}_{sp}(i-j,t) = -i\left\langle T\, \widehat{N}_i^\mathrm{hh}(t)S_{i\sigma}(t)P_{j\sigma}^\dagger(0) \right\rangle.$$

The propagator $\hat{F}_{sp}$ requires an additional equation of motion, which relates $\hat{F}_{sp}$ with the propagator

$$\hat{F}_{pp} = -i\langle T\, \widehat{N}_i^\mathrm{hh}(t)P_{i\sigma}(t)P_{j\sigma}^\dagger(0)\rangle. \quad (15)$$

To truncate the infinite set of equations for the Green's functions, we apply the Hubbard-I approximation. It is a simple mean-field scheme developed in the seminal papers[17]. The applicability of Hubbard-I and related approaches has been tested in many cases (see, e.g., Refs. 17,20,21). In the Hubbard-I approach, $\hat{F}_{pp}$ is approximated by the product

$$\hat{F}_{pp} = \langle \widehat{N}^\mathrm{hh} \rangle \hat{G}_{pp} = n^\mathrm{hh}\hat{G}_{pp}. \quad (16)$$

This closes the system of equations (13), whose solution may now be written explicitly as

$$\hat{G}_{pp} = \frac{\omega + \mu + \varepsilon_\mathrm{H}}{(\omega + \mu + \varepsilon_\mathrm{H})(\omega + \mu + \hat{T}_\mathbf{k}) - n^\mathrm{H}t_0^2},$$

$$\hat{G}_{sp} = -\frac{n^\mathrm{H}t_0}{(\omega + \mu + \varepsilon_\mathrm{H})(\omega + \mu + \hat{T}_\mathbf{k}) - n^\mathrm{H}t_0^2}, \quad (17)$$

where $n^\mathrm{H} = 1 - n^\mathrm{hh}$ is the hydrogen concentration per carbon atom. These equations are obtained in the limit $U \to \infty$. Similarly, the Green's function

$$\hat{G}_{ss}(i-j,t) = -i\left\langle T\, S_{i\sigma}(t)S_{j\sigma}^\dagger(0) \right\rangle \quad (18)$$

is calculated

$$\hat{G}_{ss} = n^\mathrm{H}\frac{1 - t_0\hat{G}_{sp}}{\omega + \mu + \varepsilon_\mathrm{H}}. \quad (19)$$

In the limiting case $n^\mathrm{H} = 0$ ($n^\mathrm{H} = 1$), the Green's functions in Eqs. (17) and (19) coincide with the exact Green's functions corresponding to the Hamiltonian H_E of graphene (H_A of graphane).

When the Green's functions are known, the density of states, the electron concentration, and the energy can be calculated as a function of μ. Fixing the electron concentration $(1 + n^\mathrm{H})$ per carbon atom, we find $\mu = \mu(n^\mathrm{H})$ and the energy $E = E[\mu(n^\mathrm{H})]$ at $T = 0$.

The Hubbard-I results are presented in Fig. 1. The energy-versus-density curve has negative curvature for any n^H. This indicates the instability of the homogeneous phase toward the phase separation. The energy of the phase separated state can be found with the help of the Maxwell construction. In our case, it is simply a straight line connecting the energy of the pure graphene at $n^\mathrm{H} = 0$ and the energy of the fully hydrogenated graphane at $n^\mathrm{H} = 1$. This means that the separated phases are pure graphene and pure graphane.

The single-electron band structure of the unstable mixed graphene-graphane phase is shown in Fig. 2. It is interesting to note that the homogeneous phase has finite density of states at the Fermi energy. This is consistent with numerical results for small clusters.[10]

IV. NUMERICAL CALCULATIONS

To verify our analytic approach, we also perform exact diagonalizations of the Hamiltonian (6) on a finite honeycomb cluster containing 10×10 unit cells (200 carbon atoms). Periodic boundary conditions are used. For each n^H, hydrogen atoms are randomly distributed on the cluster, and we calculate the system energy by averaging it over 1500 configurations.

To check the reliability of the numerical results we investigate their dependence on the number of sites in the cluster (N_sites) and the number of the configurations used
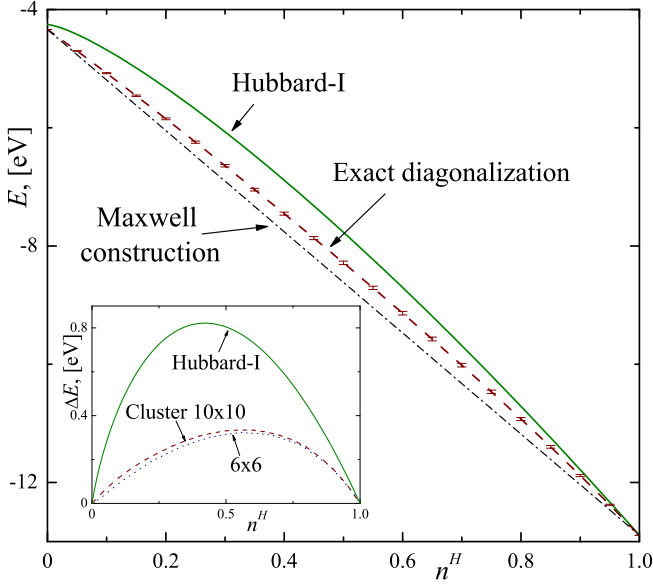
FIG. 1: (Color online) Electron energy E vs the concentration n^{H} of hydrogen adatoms calculated in the Hubbard-I approximation (green solid curve) and by exact diagonalizations of 10×10 unit cells cluster (red dashed curve). The negative curvature of $E(n^{\mathrm{H}})$ over the whole range of n^{H} is an indication of the instability of the system toward the macroscopic separation into phases with $n^{\mathrm{H}} = 0$ and $n^{\mathrm{H}} = 1$. The Maxwell construction is shown by blue dot-dashed line. The inset shows the energy difference between homogeneous and phase separated states calculated in the Hubbard-I approximation (green solid curve) and by exact diagonalizations of 10×10 and 6×6 clusters (red dashed and blue dotted curves, respectively). The model parameters are: $t_0 = 5.8\,\mathrm{eV}$, $t_p = 2.8\,\mathrm{eV}$, $\varepsilon_H = 0.4\,\mathrm{eV}$. For exact diagonalizations, $U = 400\,\mathrm{eV}$.

for the averaging (N_{config}). In Fig. 3 the averaged energy (normalized per site)

$$\langle E \rangle = \frac{1}{N_{\mathrm{config}} N_{\mathrm{sites}}} \sum_{\Theta=1}^{N_{\mathrm{config}}} E[\Theta] \qquad (20)$$

and the normalized energy dispersion

$$D_{\mathrm{E}} = \sqrt{\langle E^2 \rangle - \langle E \rangle^2} \qquad (21)$$

are plotted as functions of N_{config}. In Eq. (20) index Θ labels different realizations of disorder, $E[\Theta]$ is the energy for a given disorder realization Θ. Both $\langle E \rangle$ and D_{E} demonstrate saturation for $N_{\mathrm{config}} \gtrsim 750$. This suggests that the $N_{\mathrm{config}} = 1500$ we used in our numerical calculations is sufficient to obtain reliable results.

In Fig. 4 the same quantities are plotted versus N_{sites}. The dispersion decays as $N_{\mathrm{sites}}^{-1/2}$. This means that the relative strength of the energy fluctuations decreases when the cluster size grows, and the energy experiences self-averaging. The energy itself saturates for $N_{\mathrm{sites}} \gtrsim 125$. Therefore, our choice of $N_{\mathrm{sites}} = 200$ is adequate. In addition, the ratio $D_{\mathrm{E}}/\langle E \rangle$ sets the relative error for $\langle E \rangle$.
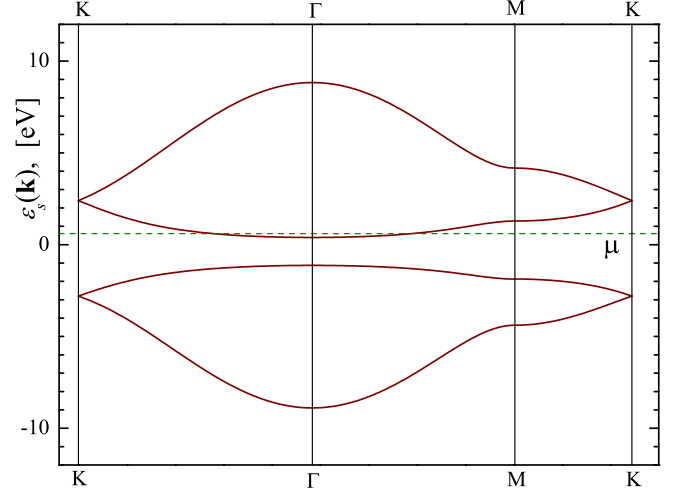

FIG. 2: (Color online) Electronic dispersion $\varepsilon(\mathbf{k})$ of the unstable homogeneous phase for $n^{\mathrm{H}} = 0.2$. Four single-electron bands, found with the help of Hubbard-I[17,22] are plotted for different points of the Brillouin zone. The chemical potential μ is marked by the horizontal green dashed line; μ was calculated self-consistently to ensure that the electron concentration is $(1 + n^{\mathrm{H}})$ per carbon atom. The gap between the conducting and the valence bands at $n^{\mathrm{H}} = 0.2$ is smaller than the graphane gap ($n^{\mathrm{H}} = 1$).
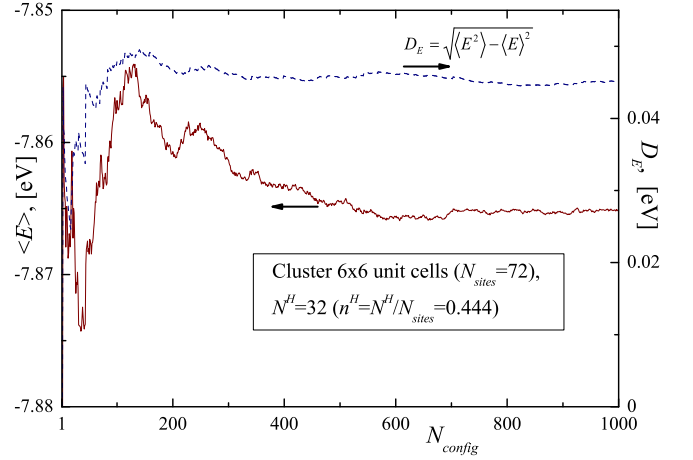

FIG. 3: (Color online) The lower (brown) curve represents the averaged energy $\langle E \rangle$, Eq. (20). The upper (blue) curve represents the dispersion, Eq. (21). The curves are plotted as functions of the number of the disorder realizations N_{config}. Both curves demonstrate saturation for $N_{\mathrm{config}} \gtrsim 750$.

For $N_{\mathrm{sites}} = 200$ this error is a fraction of a percent. We conclude that our numerical calculations are reliable.

The most important results are shown in Fig. 1, where the negative curvature of the function $E(n^{\mathrm{H}})$ is clearly seen. It implies that the system is unstable and phase separates in two phases: with $n^{\mathrm{H}} = 0$ (graphene) and with $n^{\mathrm{H}} = 1$ (graphane). Unless n^{H} is close to 0 or 1, the energy gain due to the phase separation is of the order of $10^3\,\mathrm{K}$, see the inset of Fig. 1. Thus, even at
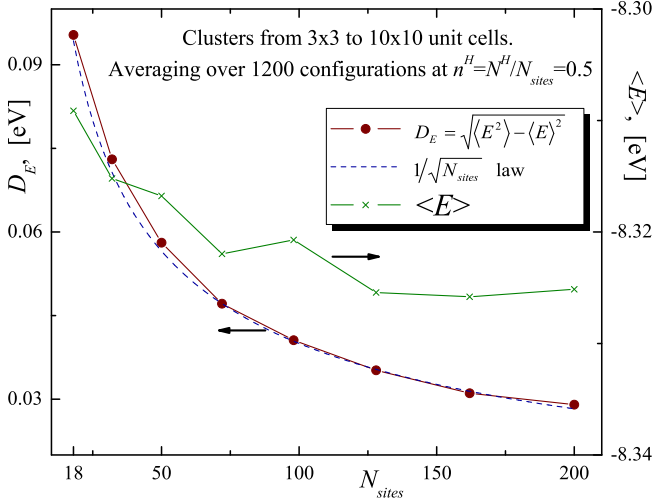
FIG. 4: (Color online) Finite size effects. The solid (green) curve (connecting skew crosses) represents the averaged energy $\langle E \rangle$, Eq. (20), versus cluster size, N_{sites}. It saturates for $N_{sites} \gtrsim 125$. The solid (red) curve connecting filled circles represents the energy dispersion, Eq. (21). It decays as $N_{sites}^{-1/2}$. The decay of the dispersion implies that for large samples the energy is a self-averaging quantity. The value of the dispersion may be used to evaluate the accuracy of the estimated value of the energy. For $N_{sites} = 200$, the error for $\langle E \rangle$ is a fraction of a percent.

room temperature we can safely use the results obtained at zero temperature.

Further, the numerically evaluated energy is of the same order as the Hubbard-I energy: the magnitude of the Hubbard-I energy is approximately two times higher than the numerical estimate (see inset in Fig. 1). Thus, the qualitative consistency between the numerical calculations and the Hubbard-I results provides firm support to the findings of Sec. III.

V. INTERFACE TENSION AND INTERFACE STABILITY

In the phase-separated state there is a boundary between graphene and graphane. The geometry of the stable inhomogeneous state depends on the sign and the value of the interface tension σ_0. If $\sigma_0 < 0$, then the inhomogeneous phase breaks into small clusters to maximize the boundary length. In the case of $\sigma_0 > 0$, the interface tension acts to minimize the length of the graphene-graphane border. In the case of a long strip this border is a straight line (if the concentration of the hydrogen adatoms is not small). However, at finite temperatures, even for positive σ_0, small thermal fluctuations destroy the perfect smoothness of the boundary between the two phases. The difference in the lattice symmetry between graphene and graphane, at the level of the electron model, manifests itself through the values of the or-

bital overlaps. In the model considered here we make an approximation regarding the orbital overlaps: we assume that several of them are equal to zero.

Further, we neglect the difference between the lattice constants in graphene and graphane. The contribution of the electron-electron interaction to the interface tension is also disregarded (we briefly discuss the effect of the interaction below). In other words, the interface tension in our model arises only due to the electron motion through the graphene-graphane boundary.

These assumptions can be justified *post factum*: (i) from our model it follows that the binding energy between a hydrogen atom and the graphene-graphane interface is of the order of t_p, which is consistent with the results presented in Ref. 9; (ii) we pointed out above that the value of the graphane gap in our simplified model Eq. (1) turns out to be consistent with other studies; (iii) we found that for intermediate hydrogenation the stable homogeneous phase has finite density of states at the Fermi energy, in agreement with Ref. 10.

We will now evaluate σ_0 in the limit shown in Eq. (8). In this approximation, electrons in graphane are localized on the C-H valence bonds [see Eq. (9)] and their contribution to σ_0 is small (this contribution is proportional to t_p^2/t_0 and ε_H). In graphene, electrons are moving from one carbon atom to its nearest neighbors. However, the electrons from graphene cannot penetrate into graphane since they have to overcome the graphane gap, which, according to Eq. (9), is of the order of t_0 when Eq. (8) holds. Thus, each carbon-carbon bond connecting an atom in graphene with an atom in graphane does not contribute to the graphene electron kinetic energy. This, in effect, is equivalent to an increase in the kinetic energy of the electrons in graphene. The longer the interface, the larger the number of "broken" bonds. Thus,

$$\sigma_0 \sim \frac{\kappa\, \varepsilon_b}{a_0}, \tag{22}$$

where ε_b is the kinetic energy for each carbon-carbon bond. The numerical coefficient

$$\kappa = \begin{cases} 1/\sqrt{3} \approx 0.6 \text{ for zigzag} \\ 2/3 \approx 0.7 \text{ for armchair} \end{cases} \tag{23}$$

characterizes the linear concentration of the carbons on the interface. The kinetic energy per bond is equal to

$$\varepsilon_b = \frac{2}{3} \int d^2\mathbf{k} \, \frac{S_0 |t_\mathbf{k}|}{(2\pi)^2} \ \sim \ t_p\,, \tag{24}$$

where the integration is performed over the first Brillouin zone, $S_0 = 3\sqrt{3} a_0^2/2$ is the area of the graphene unit cell, the factor 2 corresponds to two spin projections, $(1/3)$ enters since there are three bonds in a graphene unit cell, and $t_\mathbf{k}$ is defined by Eq. (3). After integration, we have $\varepsilon_b \approx 1.05\, t_p$, and in our approximation,

$$\sigma_0 \sim 0.6\, t_p/a_0. \tag{25}$$

A more accurate calculation (following Ref. 23) provides

$$\sigma_0 \approx 0.2 t_p/a_0 \approx 0.6\,\mathrm{eV}/a_0. \qquad (26)$$

In the calculations presented above, the contribution of the electron-electron interaction to σ_0 is disregarded. The detailed account of the interaction goes beyond the scope of the present study. Yet, we would like to offer two observations. First, the contribution due to the interaction is of the same order as σ_0. Indeed, the latter originates mostly from the energy of C-C bond. The chemical energy of C-H bond is of the same order (few eV). Thus, there is no energy scale in the system which would be able to generate an overwhelmingly large contribution to the interface tension. Second, the contribution due to the interaction increases the tension. To prove this, let us neglect the interaction in the bulk, as it is usually done for graphene, but retain the interaction term for the electrons near the graphene-graphane edge. This assumption mimics the relative importance of the interactions for electrons in lower dimensions. It is known that repulsive interaction gives positive contribution to the electron energy (see, e.g., Sec. I, § 6 of Ref. 24) and, consequently, to the interface tension.

We neglect the effects of the temperature T on the phase separation since the characteristic energies of the problem are much higher than $k_B T$ for any realistic T. However, the temperature fluctuations could affect the smoothness of the graphene-graphane interface even under such conditions. Following Ref. 25, we can express the average square fluctuation of the deviation u of the interface having a length L as

$$\langle u^2 \rangle = \frac{k_B T L}{2\pi \sigma_0}. \qquad (27)$$

Thus, we obtain

$$\frac{\langle u^2 \rangle}{a_0^2} \approx \left(\frac{L}{a_0}\right)\left(\frac{k_B T}{t_p}\right). \qquad (28)$$

Using the value of the carbon-carbon hopping $t_p = 2.8$ eV, we find that, at room temperature, the graphene-graphane interface remains atomically-flat ($\langle u^2 \rangle/a_0^2 \leq 1$) over distances

$$L_1 \approx 100\, a_0. \qquad (29)$$

Note that the estimated values of σ_0 and, consequently, L_1 will be larger if one takes into account the contribution to the interface tension due to the difference between lattice constants in graphene and graphane.

VI. CONCLUSION

We mapped the model of hydrogen atoms adsorbed on graphene on a Falicov-Kimball-like model. We demonstrated that this system has a strong tendency to phase separate. The thermodynamically stable state is inhomogeneous: all adatoms cluster together, forming two phases: hydrogen-saturated graphane and hydrogen-free graphene. The interface between these phases has finite and positive interface tension, which means that the boundary is stable and flat (if the number of hydrogen adatoms is not small). The estimated value of the interface tension is high and, at room temperature, the interface remains atomically flat over distances of about 10^2 lattice constants. This result may be of interest for fabricating graphene mesoscopic devices with weak edge scattering.

[1] A. H. Castro Neto, F. Guinea, N. M. R. Peres, K. S. Novoselov, and A. K. Geim, Rev. Mod. Phys. **81**, 109 (2009).

[2] D. S. L. Abergel, V. Apalkov, J. Berashevich, K. Ziegler, and T. Chakraborty, Adv. Phys. **59**, 261 (2010).

[3] A. Rozhkov, G. Giavaras, Y. P. Bliokh, V. Freilikher, and F. Nori, Physics Reports **503**, 77 (2011).

[4] X. Li, X. Wang, L. Zhang, S. Lee, and H. Dai, Science **319**, 1229 (2008).

[5] M. H. F. Sluiter and Y. Kawazoe, Phys. Rev. B **68**, 085410 (2003).

[6] A. K. Singh and B. I. Yakobson, Nano Lett. **9**, 1540 (2009).

[7] M. J. Schmidt and D. Loss, Phys. Rev. B **81**, 165439 (2010).

[8] L. Openov and A. Podlivaev, JETP Lett. **90**, 459 (2009).

[9] Z. M. Ao, A. D. Hernandez-Nieves, F. M. Peeters, and S. Li, Appl. Phys. Lett. **97**, 233109 (2010).

[10] T. Roman, W. A. Dio, H. Nakanishi, and H. Kasai, J. of Phys.: Cond. Matter **21**, 474219 (2009).

[11] A. V. Shytov, D. A. Abanin, and L. S. Levitov, Phys. Rev. Lett. **103**, 016806 (2009).

[12] J. K. Freericks, C. Gruber, and N. Macris, Phys. Rev. B **60**, 1617 (1999).

[13] J. K. Freericks, E. H. Lieb, and D. Ueltschi, Phys. Rev. Lett. **88**, 106401 (2002).

[14] M. M. Maśka and K. Czajka, Physica Stat. Solidi (b) **242**,

479 (2005).

[15] K. I. Kugel, A. L. Rakhmanov, and A. O. Sboychakov, Phys. Rev. Lett. **95**, 267210 (2005).

[16] A. O. Sboychakov, K. I. Kugel, and A. L. Rakhmanov, Phys. Rev. B **76**, 195113 (2007).

[17] J. Hubbard, Proc. Roy. Soc. London, Ser. A **276**, 238 (1963), *ibid.* **281**, 401 (1964).

[18] J. O. Sofo, A. S. Chaudhari, and G. D. Barber, Phys. Rev. B **75**, 153401 (2007).

[19] S. Lebègue, M. Klintenberg, O. Eriksson, and M. I. Katsnelson, Phys. Rev. B **79**, 245117 (2009).

[20] J. Beenen and D. M. Edwards, Phys. Rev. B **52**, 13636 (1995).

[21] A. V. Rozhkov and A. L. Rakhmanov, J. of Phys.: Condens. Matt. **23**, 065601 (2011).

[22] J. Hubbard, Proc. Roy. Soc. London, Ser. A **281**, 401 (1964).

[23] R. Balian and C. Bloch, Ann. Phys. (N.Y.) **60**, 401 (1970).

[24] E. Lifshitz and L. Pitaevskii, *Course of Theoretical Physics, Vol.9, Statistical Physics, Part 2* (Butterworth-Heinemann, Oxford, UK, 1999).

[25] P. Chaikin and T. Lubensky, *Principles of Condensed Matter Physics* (University Press, Cambridge, 2000).